Structural and Mechanical Properties of YBCO-Polystyrene Composites

Rosalin Abraham,[1,2] Selvin Thomas P,[3] Soosy Kuryan,[4] Jayakumari Issac,[5] K Nandakumar,[6] Sabu Thomas[2]

[1]*Department of Physics, St. Dominics College, Kanjirapally, Kottayam 686512, Kerala, India*
[2]*School of Chemical Sciences, Mahatma Gandhi University, Kottayam, Kerala, India*
[3]*Department of Chemical Engineering, King Fahd University of Petroleum & Minerals, Dhahran, 31261, Saudi Arabia*
[4]*Department of Physics, St Stephen's College, Kollam, Kerala, India*
[5]*Department of Physics, CMS College, Kottayam, Kerala, India*
[6]*Centre for Nanoscience, Nanotechnology Mahatma Gandhi University, Kottayam, Kerala, India*

Received 21 August 2008; accepted 5 February 2009
DOI 10.1002/app.30256
Published online 28 May 2010 in Wiley InterScience (www.interscience.wiley.com).

ABSTRACT: Microcrystalline powders of yttrium barium copper oxide [$YBa_2Cu_3O_7$] have been prepared by conventional ceramic preparation technique. The powder belong to orthorhombic symmetry with unit cell dimensions '*a*'=3.8214 Å, '*b*'=3.8877 Å and '*c*'=11.693 Å. XRD and SEM studies revealed that its particle size is in the micrometer range. Micro composites of polystyrene with different loading of yttrium barium copper oxide fillers were prepared by melt mixing in a brabender plasticorder at a rotor speed of 60 rpm. The lattice parameters of the constituent phases are the same in all the composites. Mechanical properties such as stress–strain behavior, Young's modulus, and tensile strength were studied as a function of filler loading. Addition of filler enhances the Young's modulus of the polymer. Because of the poor filler-matrix adhesion, tensile strength and strain at break decreases with filler loading. To explore more carefully the degree of interfacial adhesion between the two phases, the results were analyzed by using models featuring an adhesion parameter. Finally experimental results were compared with theoretical predictions. © 2010 Wiley Periodicals, Inc. J Appl Polym Sci 118: 1027–1041, 2010

Key words: composites; polystyrene; mechanical properties; Young's modulus; tensile strength

INTRODUCTION

Today, we are familiar with a large series of "high-temperature superconductors" based on copper oxide. The most studied one is $YBa_2Cu_3O_{7-\delta}$. When 'δ' is equal to zero, the substance is a perfect superconductor with orthorhombic symmetry of unit cell parameters, ($a \neq b \neq c$, $\alpha = \beta = \gamma = 90^\circ$) and when '$\delta$' is equal to one, the substance is a perfect semiconductor with tetragonal symmetry ($a = b \neq c$, $\alpha = \beta = \gamma = 90^\circ$). It is denoted as "Y123" (because of the stoichiometry of the elements) or as "YBCO" (because of the initial letters of the elements). The practical application of high-temperature superconductors for electronic applications required the development of novel processes and devices. The development of capacitors that are compatible with superconducting and manufacturing materials capable of high frequency operations will be required for integrated devices.

Hard and brittle high 'T_c' superconducting ceramics can be incorporated into polymer matrices[1,2] to produce composite materials with superior mechanical properties, greater processability, and flexibility. They can be easily molded into various useful shapes by versatile polymer processing techniques such as compression, extrusion, and injection molding. In particular, (0–3) type composites, in which superconducting ceramic powders embedded in polymer matrices, are extremely flexible.

The unique combination of good dielectric and mechanical properties is hard to achieve in a one-component material. Pure polymers are easy to process into mechanically robust components but generally suffer from low dielectric constant.[3,4] On the other hand, typical high-K materials, such as ceramics, are brittle and require high-temperature processing,[5] which are often not compatible with current circuit integration technologies. The ideal solution would be the materials that is mechanically robust and process at ambient temperatures have to be incorporated with suitable polymers such as ceramic/polymer composites that may combine desired properties of the components.[6,7]

Composites of polymers with particulate fillers have generated considerable interest because of their desirable improvement in certain properties for various applications. The performance of a composite material is strongly dependent on the combined

Correspondence to: S. Thomas (sabupolymer@yahoo.com or sabuchathukulam@yahoo.co.uk).

effects of filler particle size, filler surface chemistry, and volume fraction of the filler.[8–11]

Fillers play an important role in modifying the mechanical properties of various polymers. The Young's modulus of a polymer appears to be significantly dependent on the particle size, packing fraction, and the adhesion between the filler and the polymer.The theory of filler reinforcement of polymers predicts the formation of boundary layer of a matrix material on the surface of the filler. In some cases, the filler can improve some properties while degrading other, as in nylon-6,6, which has improved stiffness but reduced impact strength when filled with 30% glass.[12] The most important feature that affects the interfacial adhesion is believed to be the formation of boundary layers

In the present work, the effect of superconducting ceramic material, YBCO on the mechanical properties of the composites of amorphous polystyrene has been investigated. The filler used was prepared by conventional ceramic preparation technique. The objective of this article is to analyze tensile modulus, tensile strength, and elongation at break data of YBCO/PS composites on the basis of existing theoretical predictions for two-phase systems. The reinforcement behavior and the adhesion parameter of the composites were discussed from the microscopic point of view.

EXPERIMENTAL

Preparation of YBCO

Solid-state reaction technique was adopted for the preparation of the material. The starting materials were $BaCO_3$ (Merck Ltd., Mumbai, India), Y_2O_3 (CDH, New Delhi, India), and CuO(Merck Ltd., Mumbai, India). In order to prepare 15 g of $YBa_2Cu_3O_{7-\delta}$, 2.26952 g of Y_2O_3, 7.93356 g of $BaCO_3$, and 4.79685 g of CuO were required. The constituent oxides were mixed in stoichiometric ratios [as in eq. (1)] in an agate mortar and calcined at a temperature of 930°C. This step was repeated twice. Calcinations promote the decomposition of carbonates leading to the formation of the desired phase of the superconducting YBCO compounds. By each intermediate grinding, the quality of the end product was expected to improve. Then the material was reground and sintered in air at 930°C for 15 h. The grinding and sintering was repeated in oxygen and finally the material was annealed in oxygen at 500°C for 10 h.[13] Two stages were required to synthesize the 92K superconducting material. First, the basic structure must be formed at the temperature above 700 K. The tetragonal structure so formed is deficient in oxygen and does not possess superconducting properties. Accordingly, second part of the synthesis involves annealing under oxygen at a temperature 500°C. The arrangement of additional oxygen in the lattice causes a conversion from tetragonal to orthorhombic symmetry that supports superconductivity. During the annealing process, a structural transition of the 1-2-3 compound from tetragonal to orthorhombic crystal symmetry take place with varying oxygen deficiency parameter 'δ' from 0.5 to 0 where 'δ' is the variable oxygen content.

$$(Y_2O_3) + 4(BaCO_3) + 6(CuO) \rightarrow -2YBa_2Cu_3O_{7-\delta} + 4CO_2 \quad (1)$$

Composite preparation

The melt mixing technique was chosen for preparing the composites because it is a solvent free technique. By melting at high temperature, molten polystyrene can easily penetrate between filler particles, which facilitate suitable mixing and allow avoiding air trapping into the composites. Consequently void free composites were obtained. The specific properties of polystyrene are reported in Table I. YBCO/Polystyrene composites were prepared in a brabender plasticoder. The cavity for mixing in the instrument has an internal volume 40 cm^3 and is fitted with two screw type rotors of variable speed. Filling the internal cavity with 90% of mixing charges ensures a constant ram pressure and a good mixing. The temperature of the internal mixer was raised to 180°C and then polymer was added; complete melting of polymer was ensured by a constant minimum torque and reattainment of the desired cavity temperature of 180°C. YBCO powder was then added to the molten polymer and was mixed for about 6 min at a rotor speed of 60 rpm.This time was sufficient to generate a steady state torque response, indicative of uniform dispersion of the components.[14] The compositions of the fillers were 0, 10, 20, 30, and 40% by the volume fraction of the filler. The mixed samples were compression molded into sheets of desired thickness by hydraulic press at a temperature of 180°C and were used for different studies. The composites were named as YBCO10, YBCO20, YBCO30, and YBCO40.

TABLE I
Properties of Polystyrene

Properties	Value
Dielectric constant	2.5–2.65
Poisson's ratio	0.333
Water absorption	0.05%
Glass transition temp	108°C
Average molecular wt.	208,000

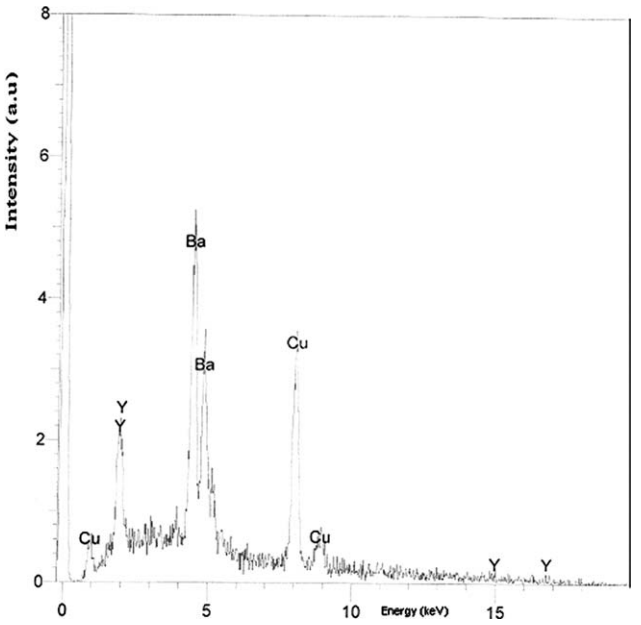

Figure 1 EDX spectrum of YBCO.

Measurements

Powder X-Ray diffraction data were taken with Bruker X–Ray diffractometer using Cu-Kα (1.5404 Å) (D8 Advance). The Bragg angles recorded on the *x*-axis were scanned from 10° to 90° in small steps. The morphology and microstructure of the composites were analyzed by means of high resolution scanning electron microscope (SEM) using a JEOL JSM 840-microscope.

Rectangular samples of 10 cm × 1.2 cm × 0.2 cm were cut for tensile testing. Tensile testing were done using a universal testing machine (FIE) at a cross-head speed of 10 mm/min. Tensile properties were determined according to ASTM D638.

RESULTS AND DISCUSSION

EDX analysis

The EDX spectrum of YBCO gave the information on the elemental composition of the material. This technique is generally associated with SEM. In this technique an electron beam of 10–20 keV strikes the surface of a sample, which causes X-ray to be emitted from point of incidence. The energy of the characteristic X-ray emitted from the different elements is different and thus it gives the unavoidable signature of the particular element.[15] The X-ray spectrum obtained gives elemental compositions of the material under investigation as in Figure 1. The percent of the elemental composition as in Table II agrees with the stoichiometric relations of $YBa_2Cu_3O_7$ and with Figure 1. The three dominant peak positions at 2, 4.6, and 5.1 keV and 8 and 8.75 keV correspond quite well to the energy pattern of the corresponding materials (Yttrium, Barium, and Copper) reported in the EDX international chart, giving the evidence that Barium is dominant in YBCO samples.

TABLE II
Material Content (YBCO)

Material	Content (wt %)
Y_2	15.132
Ba	52.88
Cu	31.98

XRD analysis

The Y (123) material crystallizes in an orthorhombic structure with space group P_{mmm}. The structure can be viewed as a defect perovskite. The basic relation for indexing an X-ray powder pattern is given by

$$\frac{1}{d^2_{hkl}} = \frac{h^2}{a^2} + \frac{k^2}{b^2} + \frac{l^2}{c^2} \quad (2)$$

The *d*-spacing of a set of planes is defined as the perpendicular distance between any pair of adjacent planes in the set and it is this '*d*' value that appears in Bragg's law. The *d*-spacing of the lines in a powder pattern are governed by the values of unit cell parameters (*a*, *b*, *c*, α, β, γ), provided the various lines have been assigned Miller indices [*hkl*]. The lattice parameters are '*a*'=3.8214 Å, '*b*'=3.8877 Å, and '*c*'=11.693 Å, obtained using the computer file PDF match to JCPDS data attached to the system analyzer and by a computer programme pdp1.1.[16]

The XRD pattern of pure YBCO is given in Figure 2. All the major peaks with intensity percent greater than 40 are listed with [*hkl*] indices corresponding to their '2θ' values. The observed and calculated '*d*' spacing is given in the fourth and fifth column of Table III. From the examination of (Δ*d*) values, it is evident that the observed and calculated '*d*' values are nearly equal for all the peaks and so the lattice parameters fit the experimental data. The calculated values of lattice parameters for YBCO, which are in close agreement with the values reported in the literature.[17] X-ray powder diffraction may be used to measure the average crystal size in a powdered sample, provided the average diameter is less than about 2000 Å. The lines in the powder diffraction are of finite breadth but if the particles are very small the lines are broader than usual. The broadening increases with decreasing particle size. The limit is reached with particle diameters in the range roughly 20–100 Å; then the lines are so broad that they effectively 'disappear' into the background radiation. For particles that are markedly non-spherical, it may be possible to estimate the shape since different lines in

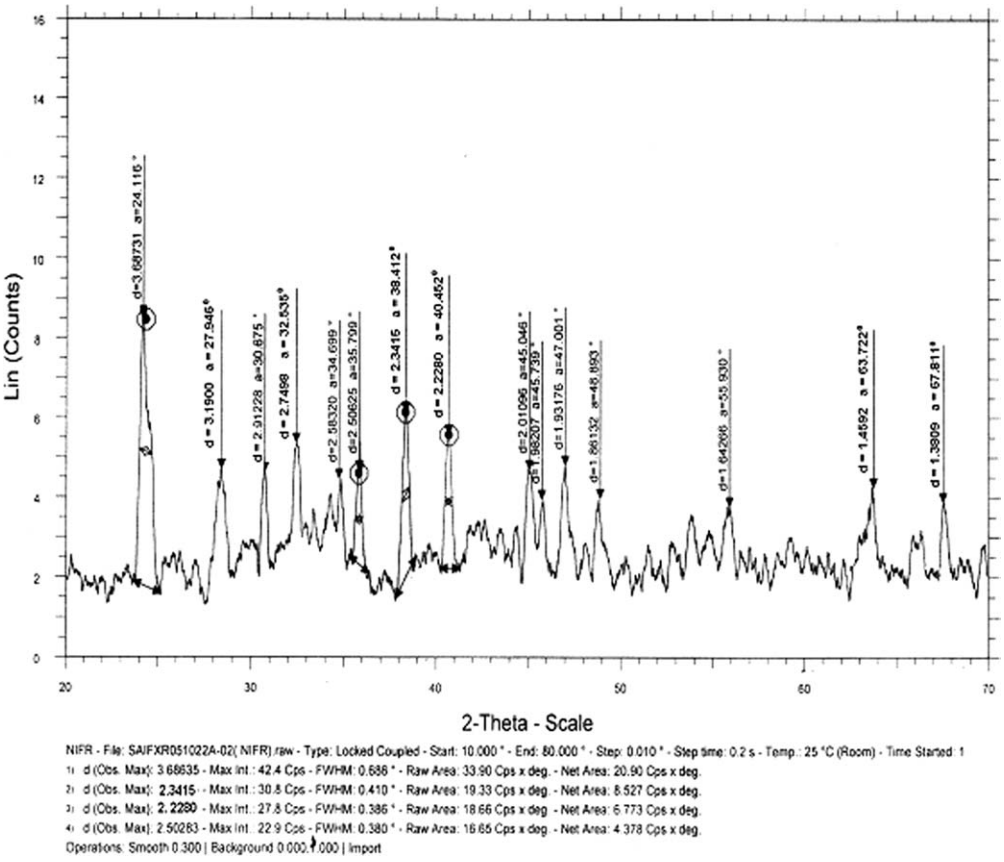

Figure 2 XRD of YBCO.

the powder pattern are broadened to differing degrees. Since XRD is a first hand measuring technique for particle size calculations, one can prefer measurement using SEM for microparticle characterization.

Characterization of the composites

The chemical non-reactivity of the filler and the polymer at the processing temperature is another important factor in the preparation process. Since the same powder was used to make all composites, the particle size was same for all concentrations. The ceramic particles appear to be well dispersed in both low and high concentration composites. Clustering or agglomeration is seen to be absent in all composites. Characterization of the composites by XRD allows identification of the crystalline components [Fig. 3(a–e)].

TABLE III
XRD Data of YBCO

Angle (2θ)	Intensity Count (%)	Intensity (%)	'*d*' observed	'*d*' calculated	*d*(cal)−*d*(obs) (Δ*d*)	[*hkl*]
24.116	8.58	100	3.68731	3.689138	0.001828	[011]
27.946	5.61	65.4	3.1900	3.1987	0.0087	[102]
30.675	5.45	63.4	2.91228	2.9232	0.01092	[004]
32.535	4.62	53.8	2.7496	2.725276	−0.024324	[110]
34.699	4.68	54.5	2.58320	2.60414	0.02094	[111]
35.799	6.14	71.6	2.50625	2.47009	−0.03616	[112]
38.412	5.6	65.2	2.3415	2.3386	−0.0029	[005]
40.452	4.69	54.6	2.228	2.233	0.005	[113]
45.046	4.24	49.4	2.01096	1.994718	−0.012648	[105]
45.739	3.76	43.9	1.98207	1.993378	0.017582	[114]
47.001	4.24	49.4	1.93176	1.994718	0.012648	[105]
48.893	4.8	55.9	1.86132	1.8910	0.02968	[200]
55.93	3.97	46.2	1.64266	1.645474	0.002814	[212]
63.722	4.46	52	1.4592	1.461625	0.002425	[008]
67.811	4.5	55	1.3809	1.362638	−0.0183	[220]

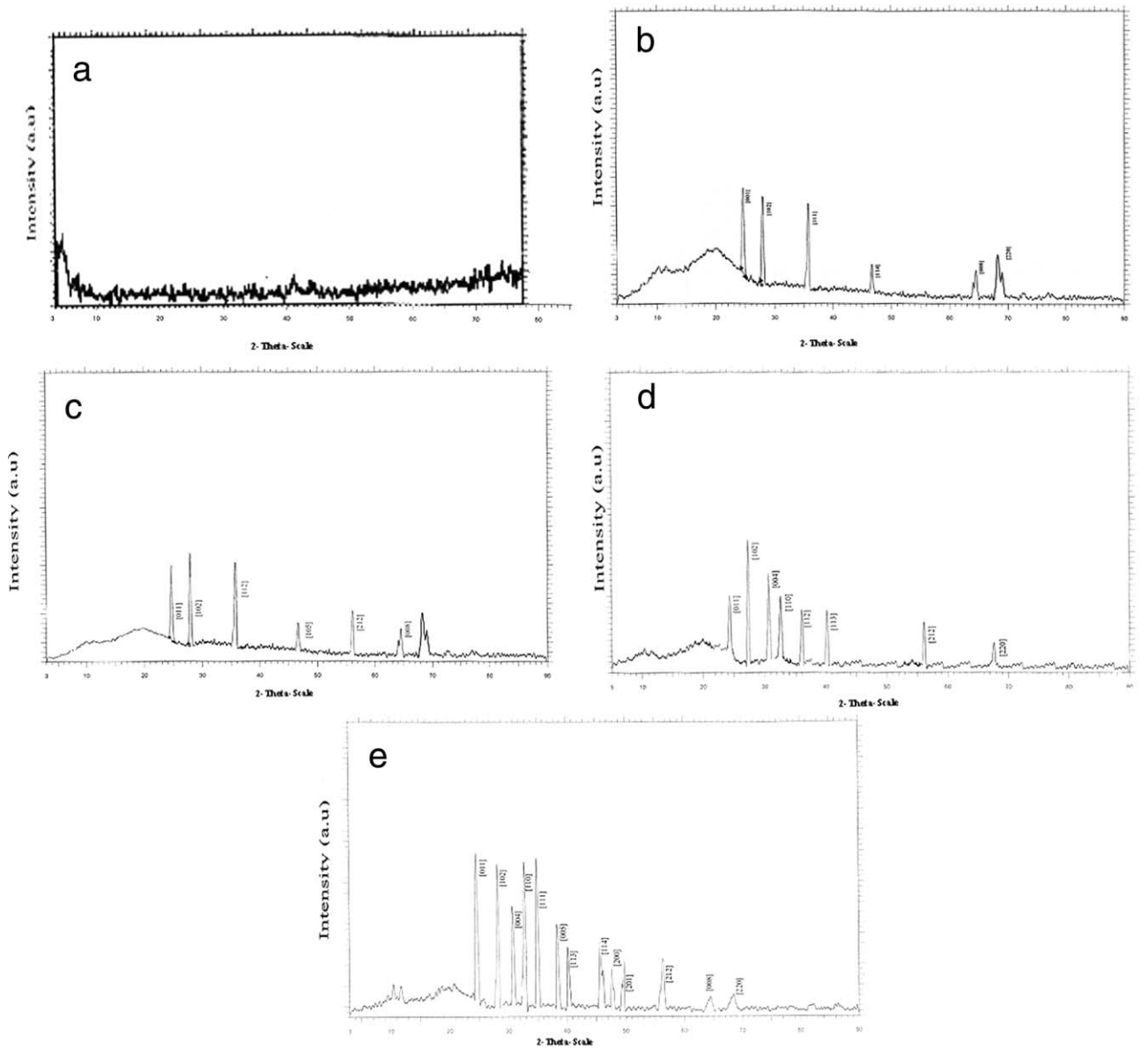

Figure 3 (a–e) X-ray diffraction patterns of polystyrene & composites.

The basic peaks of YBCO at 24.116°, 27.946°, and 35.799° were intact in the composites, indicating that the ceramic material had neither changed during the preparation of the composites, nor were the relative peak positions shifted significantly due to the presence of the polymer. For the first composite, YBCO10, strong and sharp peaks of intensity % 100 at 24.116°, intensity % 65.4 at 27.946°, intensity % 63.4 at 30.675°, intensity %71.6 at 35.799°, intensity % 55.9 at 47.001°, intensity % 52 at 63.722°, and intensity % 55 at 67.811° were present. For the second composite, YBCO20, peaks of intensity % 46.2 at 55.93° was also included. The emergence of characteristic diffraction lines and their gradual sharpening increased with filler content and for the last composite YBCO40, almost all the characteristic peaks of YBCO were present. Thus comparison of the XRD patterns of the polymer and the composites confirmed that the fillers did not react with the polymer.[17] Characterization of the composites by XRD allows identification of the crystalline components. The lattice parameters of the constituent phases are almost the same in all composites. The average particle size was estimated from these XRD lines, by Scherrer's equation and no noticeable change in particle size is observed. This indicates that the structure remains the same even if the composition of composites were varied. All the peaks of the composites were identified. No other additional peak was observed apart from the parent material. This confirms the successful preparation of the two-phase composite material.[18] The humps in the diffraction

TABLE IV
Crystal Parameters and Unit Cell Volume of YBCO and Composites

Sample	'*a*' (Å)	'*b*' (Å)	'*c*' (Å)	'*V*' ($10^{-30}m^3$)
YBCO	3.8214	3.8877	11.693	173.71654
YBCO10	3.8245	3.8871	11.695	173.86
YBCO20	3.8235	3.8875	11.6925	173.7956
YBCO30	3.8218	3.8869	11.6945	173.7212
YBCO40	3.8212	3.8875	11.6923	173.688

pattern characterize the amorphous nature of PS. They gradually gave way to discrete lines with the increment in filler content. It was observed that the characteristics peaks with high intensity were found to increase with increasing proportion of the filler. This sequence is generally consistent with the study of Panajkar et al.[19] and the recent work of Lee et al.[20] who detected the unchangability of XRD peaks of the fillers by composite formation. The unit cell parameters of YBCO particles in the composites are reported in Table IV. The unit cell parameters of the composites are same as the parent material. This indicates the absence of any chemical interaction between the filler and the matrix.

SEM analysis

Morphology has been analyzed from SEM. The filler particles are uniformly distributed in all the composites and the particles are almost spherical in shape with irregular boundaries [Fig. 4(a–e)]. In all composites, filler particles are clearly embedded in the polymer matrix. It is evidenced for the (0–3) connectivity of the composites.[21] The results give a true picture of how the fillers interact with PS matrix that effect the overall properties of the composites. The most fascinating property is the uniform dispersion of the fillers in the matrix. The surface view and fracture surface view of YBCO/PS composites revealed the dispersion of the particles in the composites [Figure 4(a–f)]. The particle dispersion and particle-matrix reinforcement play vital roles for both tensile and elongation properties of the composites. In all pictures it is seen that all the particles are neatly coated with PS and the size of the particles is less than 1 μm. The ceramic particles are dispersed homogeneously with the interspaces filled with PS, and large defects are not observed in the fracture surface view of the composites.[22] The fractured surface of the composites showed a dense microstructure as in Figure 5(a–e). SEM photographs were used to determine the size of the dispersed particle and the particle size distribution. This was done by counting a large number of particles (more than 100) from various micrographs of different magnification and quantitatively analyzed in terms of their diameter.[23] The results are reported in Table V.

The number average particle diameter,

$$\frac{\sum NiDi}{\sum Ni} = Dn \tag{3}$$

The weight average particle diameter,

$$\frac{\sum N_i D_i^2}{\sum N_i D_i} = D_w \tag{4}$$

The volume average particle diameter,

$$\frac{\sum N_i D_i^3}{\sum N_i D_i^2} = D_v \tag{5}$$

where 'N_i' is the number of particles having diameter 'D_i'. The polydispersity index, a measure of particle size distribution was calculated as

$$\frac{D_w}{D_n} = \text{PDI} \tag{6}$$

The calculated polydispersity index is 1.028, and the value gives clear evidences for the uniform dispersion of filler in the matrix.[24] SEM is equipped with polaroid camera for documentation. The instrument is used to provide information about the surface topography of polymers. An electron beam sweeps over the surface emitting secondary and back scattered electrons, which are used to construct image of the surface. From the SEM pictures it is clear that the size of the YBCO particle is around 650 nm.

Density calculations

The first, second, and third columns of Table VI report the density pattern of the prepared composites.

The theoretical density values were calculated using the rule of mixtures.

$$\rho_c = \rho_p(1 - v_f) + \rho_f \; v_f \tag{7}$$

where ρ_c is the density of the composite, ρ_p is the density of phase 1(polymer phase), ρ_f is the density of phase 2(ceramic phase), and 'v_f'is the volume fraction of filler. The values of ρ_p and ρ_f were taken to be 1050 kg m^{-3} and 5250 kg m^{-3} respectively.[25] First and second column of Table VI compares the average of the measured density values (by sample geometry and Archimedes methods) with theoretical values. As density measurements of YBCO/PS, it is revealed that the composite pellets followed the rule of mixtures with respect to the constituent powders, so that no change in porosity is induced by the thermal processing. Lee and Chen studied the density variations in ceramic superconductor (2223)-nylon 6,6 composites and they got a variation of bulk density of 2223-nylon 6,6 composites with volume fraction of 2223 filler.[26]

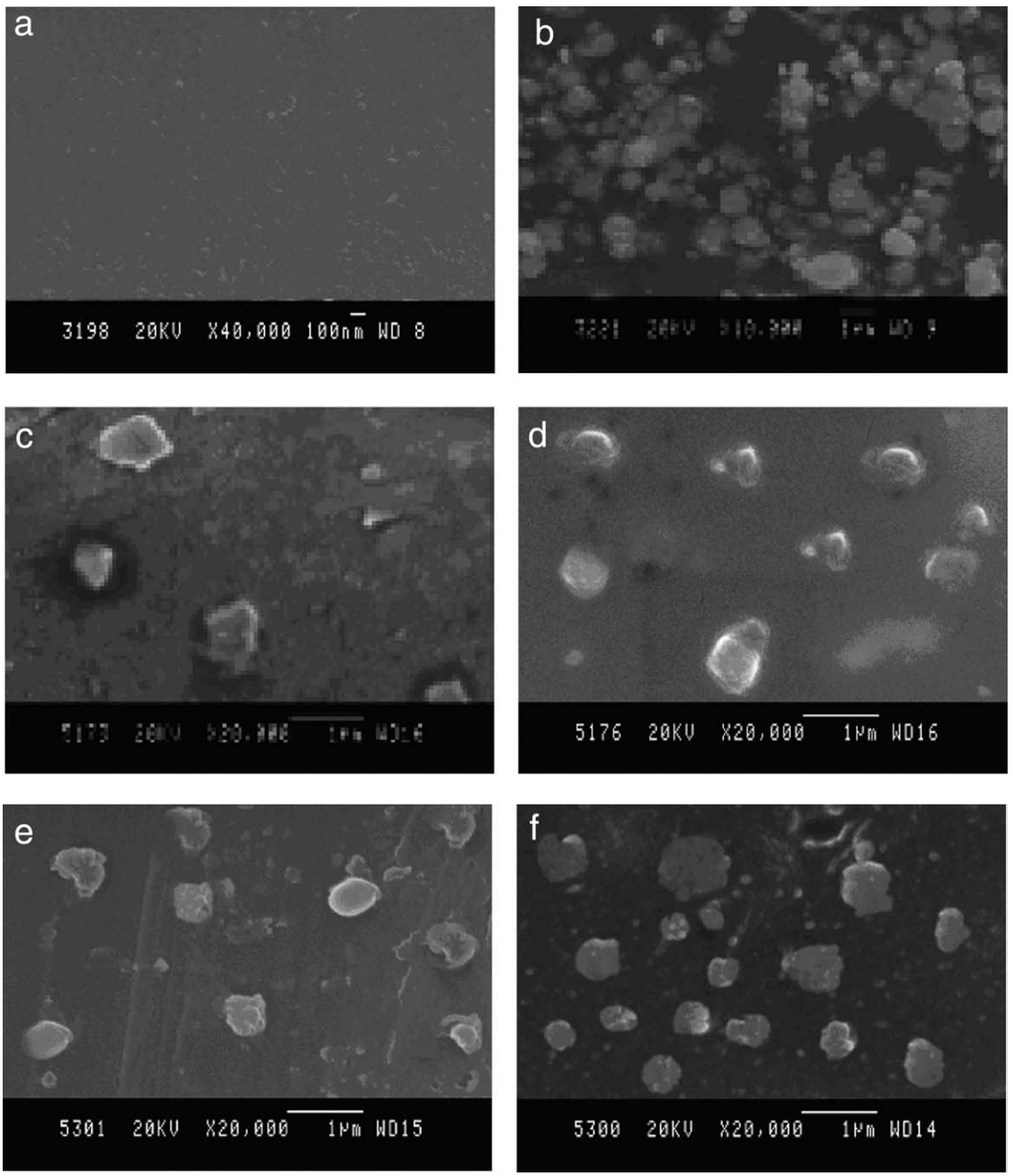

Figure 4 (a–f) Surface view of PS, YBCO, and composites.

Stress–strain behavior of PS and composites

There is a large body of literature that discusses the mechanical property behavior of filled polymer systems. These reports reveal that the tensile modulus is the easiest property to estimate because it is a bulk property that depends primarily on the geometry, particle size distribution, and concentration of the filler. The two principal parameters used to describe the mechanical behavior of polymer is its stress and strain behavior. In the initial stages of the stress, the strain increases linearly (Hookean region). Modulus is the ratio of the stress to strain in the linear region of the stress–strain curve. It is well known that the modulus increases for a polymer when mineral filler is incorporated into it. The exact nature of the tensile response of a polymeric material depends upon the chemical structure of the polymer, conditions of the sample preparation, molecular weight, molecular weight distribution, crystallanity, and the extent of any cross-linking or branching.[27]

At normal temperature and pressure, polystyrene exhibits an increase in stress with increasing strain up to the point of sample failure. The stress at failure is called ultimate stress or stress at break. Figure 6 shows the stress-strain behaviour of polystyrene

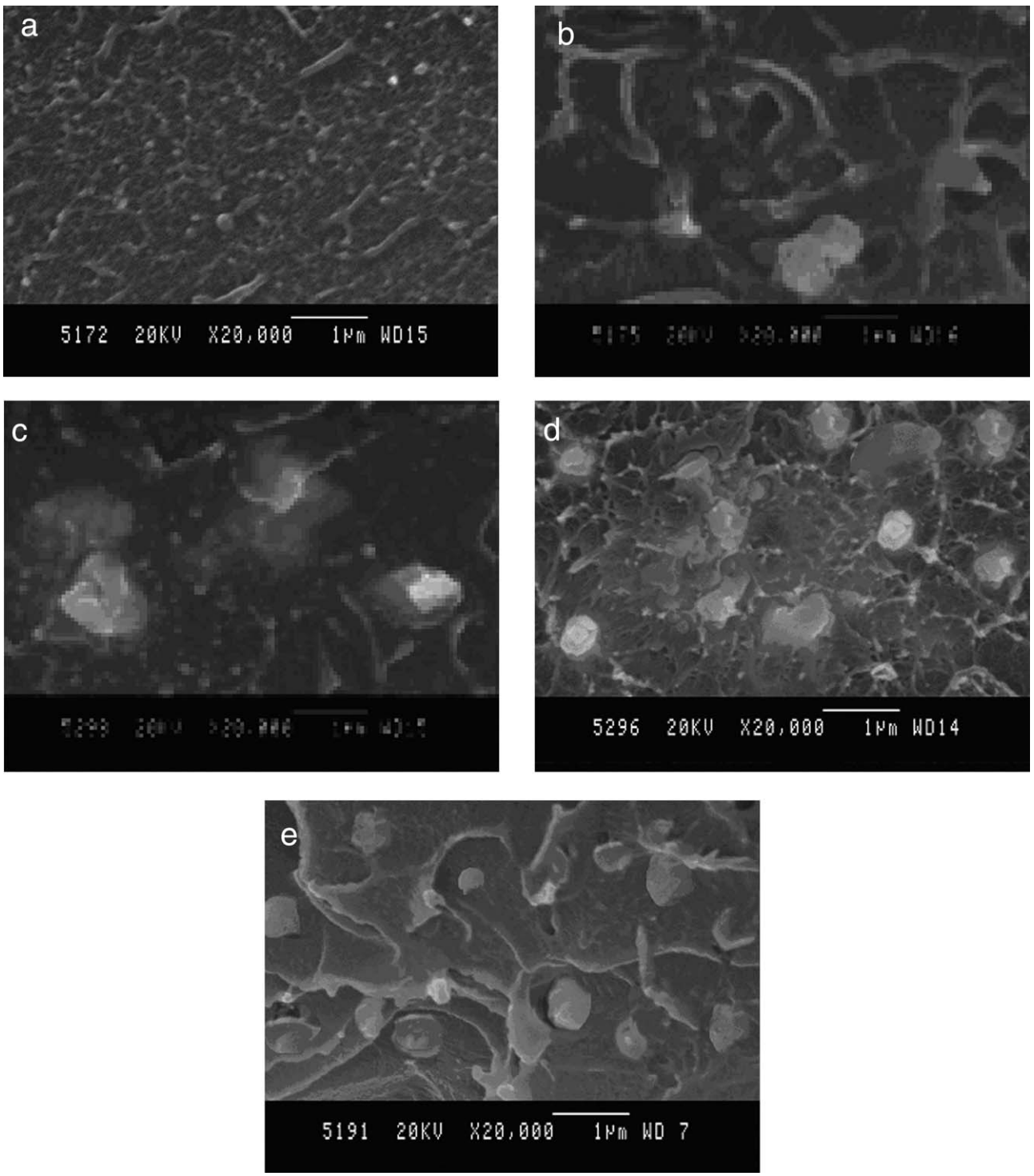

Figure 5 (a–e) Fracture surface views of polystyrene and composites.

and its composites. Typical value of modulus, ultimate stress and strain at break of the PS, and composites are shown in the last three columns of Table VI.

Theoretical modeling of tensile modulus

The mechanical properties of two-phase composites made up of particulate filled polymer phase have been studied in great detail. As a result, a variety of models are available to describe the modulus, tensile strength, and elongation at break as a function of filler volume fraction. The modeling and simulation of polymer-based composites has become an important topic in recent times because of the need for the development of these materials for engineering applications.

TABLE V
Particle Diameter Measurement (nm)

Name of sample	Number average	Weight average	Volume average	PDI
YBCO	684.75	694.76	698.79	1.0146
YBCO10	662.5	699.6	715.21	1.055
YBCO20	678	685.06	698.12	1.0103
YBCO30	562.5	587.78	611.342	1.0444
YBCO40	662.5	678.25	689.96	1.0165

The mechanical properties of particulate filled composites are affected by a number of parameters such as filler orientation, particle size of the filler, and filler/matrix adhesion etc. The load transfer from matrix to filler in a composite is strongly related to optimum mechanical properties of the composites. Several theories have been proposed to model the tensile modulus of 'the non-interactive' composite materials in terms of different parameters. Among the most prominent, historically and technically are those developed by and Sato and Furukawa,[28] Kerner,[29] Quemeda,[30] and Thomas et al.[31] These theoretical predictions are neatly correlated with the experimental values and graphically represented in Figure 7.

Sato and Furukawa

Sato and Furukawa have developed an expression for the modulus for the case where the adhesion is so poor. The equation is

$$\mathrm{M_c} = \mathrm{M_m}\left[\left(1+\frac{v_f^{2/3}}{2-2v_f^{1/3}}\right)(1-\psi \mathrm{j}) - \frac{\mathrm{v_f}^{2/3}\psi \mathrm{j}}{(1-\mathrm{v_f}^{1/3})\mathrm{v_1}}\right] \quad (8)$$

where 'M_c' and 'M_m' are the Young's modulus of the composite and the matrix respectively

$$\psi = \left(\frac{\mathrm{v_f}}{3}\right)\frac{1+\mathrm{v_f}^{1/3}-\mathrm{v_f}^{2/3}}{1-\mathrm{v_f}^{1/3}+\mathrm{v_f}^{2/3}} \quad (9)$$

and v_1 is the volume fraction of filler. 'j' is the adhesion parameter, $j = 1$ for poor adhesion, and $j = 0$ for perfect adhesion. For modeling purpose, the value of j is taken as 0.35 and plotted in Figure 7.

Kerner equation

Kerner equation can be used to estimate the modulus

$$\mathrm{M_c} = \mathrm{M_m}\left[1+\frac{v_f 15(1-r)}{V_m(8-10r)}\right] \quad (10)$$

where V_m is the matrix volume fraction and 'r'is the Poisson's ratio of the matrix. For expansible polymers incorporating rigid spherical particles featuring poor adhesion, the Kerner equation can be used to estimate the modulus.

Quemeda equation

$$\mathrm{M_c} = \mathrm{M_m}\left[\frac{1}{(1-0.5Kv_f{}^2)}\right] \quad (11)$$

where K is a constant normally 2 for non-interactive micro fillers. This variable coefficient is introduced to account for the interparticle interactions and difference in particle geometry. For filled polymers with micro particles, 'K' is taken as 2.

Thomas equation

$$\mathrm{M_c} = \mathrm{M_m}(1+2.5\,v_f+10.05\,v_f{}^2 + 0.00273\exp[16.6\,v_f] \quad (12)$$

Thomas equation is an empirical relationship based on the data generated with dispersed spherical particles in polymer matrices.

It can be seen that the experimental results are placed in between Sato Furukawa and Quemeda relations. All these predictions assume that the matrix and filler have no appreciable degree of interaction. Any interaction operative would only be physical. The polymer matrix is stiffened by the particulate. In most conventionally filled polymer systems the modulus increases linearly with the filler volume fraction. The enhancement of the modulus for YBCO/PS may not be attributed simply to the introduction of the high modulus inorganic filler to PS matrix.

TABLE VI
Some Representative Properties of the Composites

Name of the sample	Theoretical density (kg m^{-3})	Observed density (kg m^{-3})	% Error (density values)	Ultimate stress (MPa)	Strain at break (%)	Young's modulus (GPa)
Polystyrene	1050	1050		23.6	1.277	1.838
YBCO10	1470	1465	0.34	21.39	1.111	1.967
YBCO20	1890	1870	1.05	19.656	0.992	2.0713
YBCO30	2310	2300	0.4	18.5	0.876	2.1684
YBCO40	2730	2725	0.1	16.181	0.707	2.3998

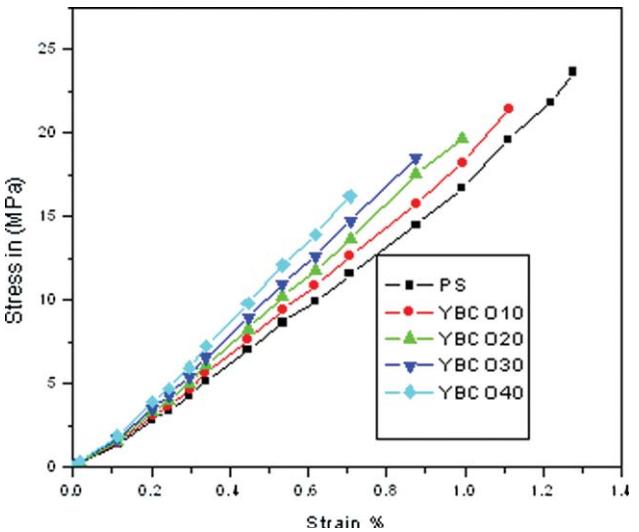

Figure 6 Stress–strain curves of YBCO/PS composites. [Color figure can be viewed in the online issue, which is available at www.interscience.wiley.com]

The increase of modulus is mainly governed by the particle size of the filler. The explanation is based on the assumption of a special morphology of the polymer matrix around the filler particles. When a thermoplastic is cooled down from the melt a solidification process will take place. During cooling from the processing temperature of the composites (180°C) to room temperature the filler particles are assumed to act as sites where thermal contraction is particularly favored, which should cause the special morphology. If it is assumed that the polymer adjacent to the embedded particles contract in an earlier stage of process because of the difference in thermal conductivity of the polymer (0.1–0.2 W/m/K) and that of ceramics is (~1– 40 W/m/K), a zone with a higher density (high modulus) will be formed around the filler particle. Because of the heat transportation processes, a depletion zone with relatively low density (low modulus) will be created surrounding the high-density zone. It is essentially due to the different thermal expansion of polymer (50×10^{-6} K^{-1} to300×10^{-6} K^{-1}) on one hand and ceramics (0.5×10^{-6} K^{-1} to15×10^{-6} K^{-1}) on the other hand[32] According to Van Krevelan[33] Young's modulus (E) is proportional to the seventh power of density (ρ).

This means that the starting zones, which have a higher density, have a higher Young's modulus, and the depletion zones, which have a lower density, have a lower modulus. The filler particles can act as initiation sites of the solidification process, and for this reason they could be surrounded by an enriched layer of polymer with an increased modulus (high modulus layer), around which a zone of material with a lower modulus is found.[34]

The effect of this morphology on the Young's modulus of the filled polymer with respect to the filler particle size will cause a combination of both effects. Two extremes are treated: a polymer filled with very small particle (nano particle), and a polymer filled with very large particles (size>10 μm). Of course, an intermediate particle size will cause a combination of both effects. In the case of composite material filled with nano particles, the interparticle distance is so small and by the abundance of number of particles there is a huge number of starting points for thermal contraction process, so that a homogeneous matrix material of 'high modulus' polymer is assumed to be created around the filler particle (Figs. 8,9). For a large filler particle the thickness of high modulus layer is very small compared to the diameter of the filler particle. On the other hand, from calculations of Matonis and Small[35] it appears that even a very thin layer of low modulus material surrounding a filler particle has a significant lowering effect on the Young's modulus of the composite.

A combination of these two effects leads to the conclusion that in the case of small filler particles the described morphology has an increasing effect on the Young's modulus of the material and for a large filler particle, the vice versa. So it is assumed to have an increasing effect on the Young's modulus for YBCO/PS, since the particle size of YBCO lies between the two extremes (of the order of 650 nm). By linear fitting the initial portions of stress–strain curves (Hookean region) (Fig. 6), it is observed that all YBCO/PS composites showed an increment in Young's modulus with respect to virgin PS. In order

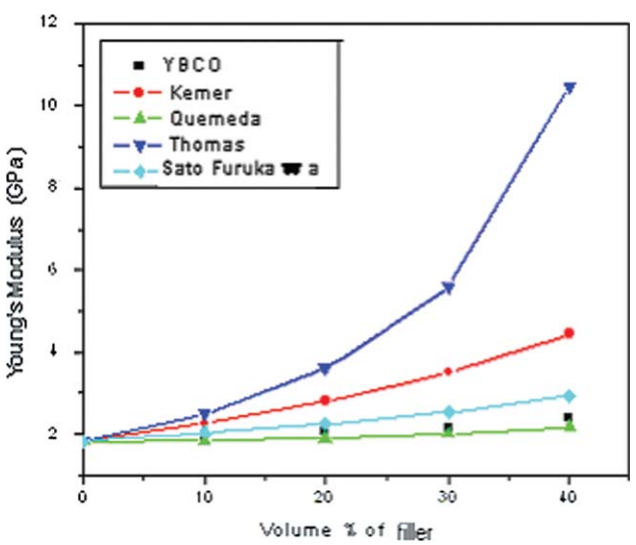

Figure 7 Theoretical modeling of the tensile modules of YBCO/PS composites. [Color figure can be viewed in the online issue, which is available at www.interscience.wiley.com]

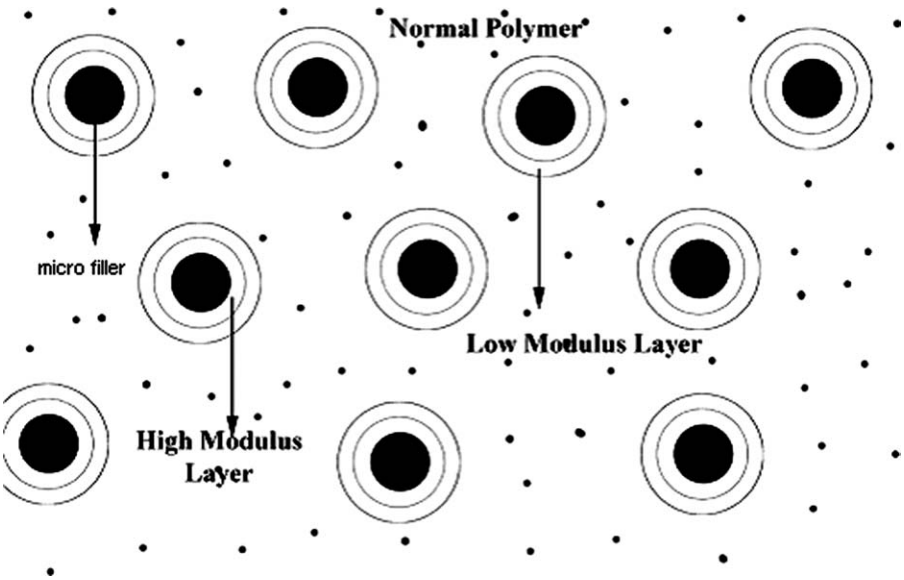

Figure 8 Proposed morphology of the polymer matrix with micro size filler particles.

to find out whether this hypothesis explains not only qualitatively but also quantitatively the observed differences in Young's moduli, some calculations were performed, using filled samples with Sato and Furukawa relations. With Sato and Furukawa relations, Young's modulus can be calculated with an adhesion parameter $j = 1$ for poor adhesion, $j = 0.5$ for medium adhesion, and $j = 0$ for good adhesion. The experimental data for various volume fractions of YBCO/PS is found to be less than that with the case of $j = 1$ as IN Figure 10.

From the above discussions it could be argued that the particle size play an important role in Young's modulus value. Generally, the elastic modulus increases with augmenting filler volume fraction, while all other tensile properties such as the ultimate stress and strain at break decreases with increasing filler volume fraction.[36] As expected, the elastic modulus is enhanced and the tensile stress decreased with increasing filler concentration in the case of YBCO/PS composites. The modulus enhancement is normally expected in particulate composites. The observed decrease in tensile stress with increasing filler concentration is due to the weak interfacial adhesion between the fillers and PS matrix.[37] Owing to the non-polar character of PS, the interfacial adhesion between PS and filler is very poor.

However, many investigations showed that the effect of solid fillers on the tensile strength of polymers might be positive or negative, depending on such factors as filler size and shape, internal stresses, surface nature, and aspect ratio.[38] In the prepared composites, the interaction between filler and polymer is expected to be physical. The polymer matrix is, however, stiffened by the particulate. The

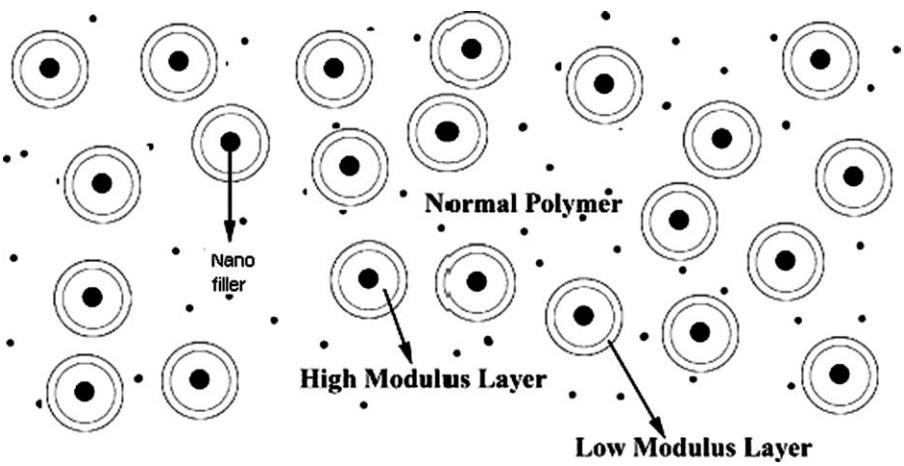

Figure 9 Proposed morphology of the polymer matrix with nano size filler particles.

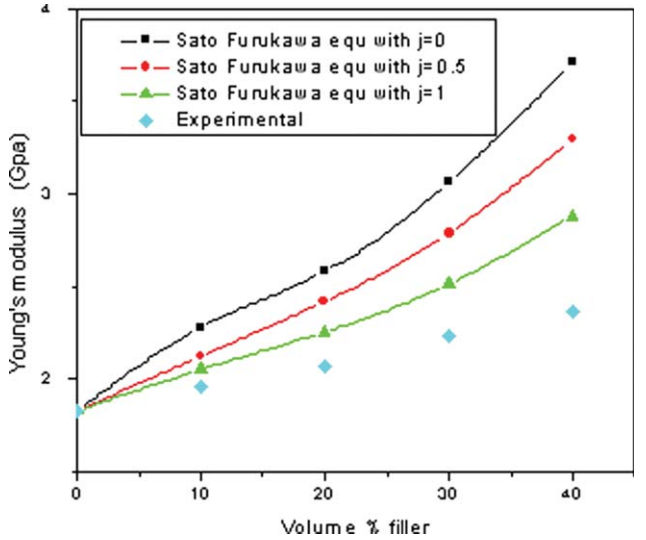

Figure 10 Theoretical modeling of the tensile modulus of YBCO/PS composites with different adhesion parameters. [Color figure can be viewed in the online issue, which is available at www.interscience.wiley.com]

particles restrict the mobility and deformability of the matrix by introducing a mechanical restraint, the degree of which depends on the particulate spacing and the properties of the particle and the matrix. Restriction in polymer molecular diffusion is seen in the presence of solid particles.The most important feature that affects the interfacial adhesion is believed to be the mechanical stresses, chemical interactions, and physico-chemical weak boundary layers.

Tensile strength

The tensile strength of a filled polymer is more difficult to predict because it depends strongly on local polymer filler interactions as well as the above factors. Tensile strength is the force required to pull the composite to the point where it breaks. Specifically, the tensile strength of a material is the maximum amount of tensile stress that it can be subjected to before failure. Brittle materials, such as PS, do not have an yield point, which means that ultimate strength and breaking strength are same. The effect of volume fraction of YBCO on tensile strength of the composites is given in Table V. The virgin PS shows a tensile strength of around 25 MPa, coincides with its reported values.[39]

Tensile strength and elongation at break value of the composites decreases with YBCO filler loading. One problem in particulate-filled composites is the poor stress transfer at the filler-polymer interface because of the non-adherence of the filler to the polymer. The micro composites showed a decrement in its ultimate stress value and strain at break value.[40]

Theoretical modeling of tensile stress

A simple model was used by Goodier[41] for the determination of tensile stresses in unfilled and filled polymer with inclusions. It is assumed that at the composite tensile stress, the polymer has undergone maximum plastic deformation. Moreover, the load carried by the components corresponds to their effective cross-sections occupied in the specimen, i.e. $(1 - (1.21)v_f^{2/3})$ for the matrix and $((1.21)v_f^{2/3})$ for the inclusions, where 'v_f' is the volume fraction of inclusions in the composites.[42] If it is assumed that the average stress acting across the surface of the fillers is £*, the following equivalence must be valid:

$$£ = £_m(1 - (1.21)\ v_f^{2/3}) + £^*((1.21)\ v_f^{2/3}) \qquad (13)$$

where, £ and $£_m$ are the composite and matrix tensile stresses, respectively. The load carried by the filler (£*) is always very much smaller than the matrix tensile stress when the filler with large particle size is used, i.e. debounding takes place. In contrast with the tensile modulus, theoretical predictions of the tensile stress are less highly developed. However, extensive work has been reported by some authors, including Nielsen,[43] Piggot and Leidner,[44] and Nicolais and Narkis.[45] All theories expose the relationship between tensile stress and volume fraction of the filler. Nicolasis and Narkis proposed that

$$£ = £_m(1 - Kv_f^{2/3}) \qquad (14)$$

where £ and $£_m$ are the tensile strength of composite and the matrix and v_1 is the volume fraction of the filler.

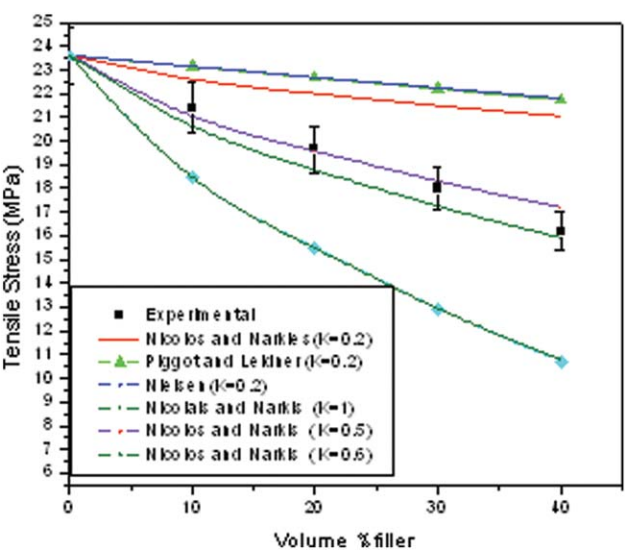

Figure 11 Modeling of tensile stress of YBCO/ PS composites. [Color figure can be viewed in the online issue, which is available at www.interscience.wiley.com]

The parameter, K, in the Nicolasis–Narkis model accounts for the adhesion between filler particles and the matrix; the lower the value, the better the adhesion. The theoretical value of K for extreme case of poor adhesion is ($K = 1.21$). For modeling in Figure 11, the value of K is taken as 0.2, 0.5, 0.6, and 1.0 for Nicolais–Narkis model.

When K=0.2, eq. (14) becomes

$$£ = £_m(1 - 0.2\ v_f^{2/3}) \quad (15)$$

When $K = 1$, eq. (14) becomes

$$£ = £_m(1 - v_f^{2/3}) \quad (16)$$

Whereas Piggot and Leidner suggested a first power relationship

$$£ = £_m(1 - B\ v_f) \quad (17)$$

The parameter B accounts for the weakness in the structure due to stress concentration. B is also taken as 0.2, eq. (17) becomes

$$£ = £_m(1 - 0.2\ v_f) \quad (18)$$

Nielsen suggested that another way of representing the tensile strength is to consider a two-phase system with poor adhesion between matrix and filler as a matrix with voids. In this extreme, the filler occupies the voids without having any influence on the mechanical properties of the composites due to the absence of adhesion at the interfacial boundary. According to the porosity theory, which has been widely used for polymeric and non-polymeric materials such as metals and ceramics,[46] the specific change in tensile strength is directly proportional to the porosity, P

$$\{- d£/£ = aP\} \quad (19)$$

where 'a' is the proportionality constant, and the negative sign represents the decrease in tensile strength with an increase of porosity. Replacing the porosity with filler volume fraction and integrating leads to the expression

$$£ = £_m \exp(- av_f) \quad (20)$$

The parameter 'a' is suggested to be related to the stress concentration; the higher the value of 'a' the greater the stress concentration effect or the poorer the adhesion. In these results 'a' is taken as 0.2, the eq. (20) becomes

$$£ = £_m \exp(-0.2v_f) \quad (21)$$

Tensile stresses of YBCO/PS composites are reduced with increasing filler volume fraction. Micro filler reduces the effective cross-section of the matrix in the loaded composite. This leads to an increase in internal stress, at any given external loading, compared with the unfilled matrix. Stress concentration caused by the filler also contributes to the internal stress. Micro plastic deformations occur around the particles, which facilitate damage of the material at lower external load, compared with unfilled PS. At the time of processing as a consequence of the different expansion coefficients, thermally induced internal stresses occur around the filler particles. This contributes to an increase of the dewetting stress.[47] Because of the increased size of the particulate filler, the high modulus layer surrounding the filler particle is very small and the stress transfer capacity is effectively reduces with the addition of filler. The experimental values are lying in between the Nicolais–Narkis predictions with $K = 0.5$ and 0.6, in the poor adhesion range. The first two experimental values for YBCO10 and YBCO20 coincide with Nicolais-Narkis predictions with K=0.5, and the tensile stress for YBCO40 coincide with Nicolais- Narkis predictions with $K = 0.6$.

Elongation at break

Normally addition of rigid particulate fillers to a polymer matrix decreases the elongation at break. Only in rare instances, if there is a good reinforcement between polymer and the filler, the fracture goes from particle to particle rather than following a direct path, and these filled polymers have nearly equal elongations at break when compared with neat polymer. Table VII shows the variation of elongation at break of the composites with fillers.

In heterogeneous polymer systems the mechanism of micromechanical deformations and consequently, the macroscopic properties of the polymers are determined by local stress distribution around the inclusions[48,49] because the non-adherence of filler to polymer, the filler particles are unable to carry any load, making it a weak body. Stress concentrations will be created around the particles, reducing the composite strength further. The elongation at break values in the filled polymer composites are generally much less than that of the polymer matrix because the filler forces the matrix to deform more than the

TABLE VII
Theoretical and Experimental Values of Elongation at Break

Name of the sample	Experimental	Calculated	Percentage error
PS	1.277		
YBCO10	1.111	0.684	38.43
YBCO20	.993	0.530	46.62
YBCO30	0.876	0.422	51.82
YBCO40	0.707	0.336	52.47

overall deformation of the composite. A basic model that describes the elongation at break was developed by Nielsen. For the case of perfect adhesion, under the assumption that the polymer breaks at the same elongation in the filled system as in the neat polymer, the elongation at break is given by

$$\epsilon = \epsilon_m(1 - v_f^{1/3}) \quad (22)$$

where ϵ and ϵ_m are the elongations at break of the composites and the unfilled polymer, and v_f is the volume fraction of the filler respectively. In the extreme case of poor adhesion, the elongation is expected to decrease as in eq. (22). An acceptable agreement between calculated and experimental data for elongation at break value is not obtained because the model is suggested for filler particle size larger than one micrometer. The probability of filler aggregation greatly increases with increasing particle size. Large filler particles strongly aggregate, leads to deterioration of elongation properties.

CONCLUSIONS

Polycrystalline YBCO ceramic powder with particle size of the order of 650 nm has been synthesized using conventional ceramic technique. Prepared composites out of it and XRD studies of the composites confirmed the successful preparation of the two-phase composite material. The morphology and tensile behavior of YBCO/PS composites were studied in detail. The filler particles are uniformly distributed in all composites and the particles are almost spherical in shape with irregular boundaries. In all composites filler particles are clearly embedded in the polymer matrix. The most fascinating property is the uniform dispersion of the fillers in the matrix. The particle dispersion and particle-matrix reinforcement play vital roles for both tensile and elongation properties of the composites. The Young's moduli of the composites increase linearly with increase of filler concentration. In order to gain more insight into this problem, a special morphology is designed for the composite phases. Tensile strength and elongation at break value of the composites decreases with filler addition. The particle size plays an important role in tensile properties of the composites. Filler reduces the effective cross-section of the matrix in the loaded composite. This leads to an increase in internal stress, at any given external loading, compared with the unfilled matrix. Stress concentration caused by the filler also contributes to the internal stress. Micro plastic deformations occur around the particles, which facilitate damage of the material at lower external load, compared with unfilled PS. At the time of processing as a consequence of the different expansion coefficients, thermally induced internal stresses occur around the filler particles. This contributes to an increase of the dewetting stress.

References

1. Dabrowski, B. Supercond Sci Tech 1998, 11, 54.
2. Saqan, S. A.; Ayesh, A. S.; Zihlif, A. M.; Martuscelli, E.; Ragosta, G. Polym Test 2004, 23, 739.
3. Hameed, N.; Thomas, S. P.; Abraham, R.; Thomas, S. Express Polym Lett 2007, 6, 345.
4. Kuryan, S.; Abraham, R.; Issac, J. Int J Pure Appl Phys 2008, 4, 33.
5. Suzhu, Y. U.; Hing, P.; Hu, X. J Appl Phys 2000, 88, 398.
6. Popielarz, R.; Chiang, C. K.; Nozaki, R.; Obrzut, J. Macromolecules 2001, 34, 5910.
7. Yoon, C.-B.; Lee, S.-H.; Lee, S.-M.; Koh, Y.-H.; Kim, H.-E.; Lee, K.-W. J Am Ceram Soc 2006, 89, 2509.
8. Kuryan, S.; Abraham, R.; Issac, J. Indian J Pure Appl Phys 2008, 46, 30.
9. Bliznakov, E. B.; White, C. C.; Shaw, M. T. J Appl Polym Sci 2000, 77, 3220.
10. Dickie, R. A. J Polym Sci Polym Phys 2003, 14, 2073.
11. Kuryan, S.; Abraham, R.; Issac, J. Int J Mater Sci 2008, 3, 47.
12. Bur, A. J. Polymer 1985, 26, 963.
13. Harris, D. C.; Hills, M. H. Chem Educ 1987, 64, 847.
14. Acosta, J. L.; Jurado, J. R. J Appl Polym Sci 1995, 47, 431.
15. Sharat Singh, N. K.; Nandakumar Sarma, H. J. Resonance 2005, 10, 61.
16. M.Calligaris, Third International School and workshop of Crystallography on X-ray powder diffraction and its applications, Cairo, Egypt, January [1990].
17. Huang, Q. W.; Wang, P.-L.; Cheng, Y.-B. Mater Lett 2002, 56, 915.
18. Takashige, M.; Kojima, S. Jpn J Appl Phys 1993, 32, 4384.
19. Panajkar, M. S.; Phatak, G. M.; Gangadharan, K.; Gopalakrishnan, I.; Gopinathan, K. J Mater Sci Lett 1997, 16, 218.
20. Lee, W. E.; Arshad, S. E.; James, P. F. J Am Ceram Soc 2007, 90, 727.
21. Zhang, T.; Tang, D.; Shao, Y.; Ke, X. J Am Ceram Soc 2007, 90, 989.
22. Mao, X.; Shimai, S.; Dong, M.; Wang, S. J Am Ceram Soc 2007, 90, 986.
23. Quintas, A.; Majerus, O.; Caurent, D. J Am Ceram Soc 2007, 90, 712.
24. Cowie, J. M. G., Ed.Polymers: Chemistry & Physics of Modern Materials; Chapman & Hall, Nelson Thornes Ltd: Delta Place, UK, 2002.
25. Abraham, R.; Kuryan, S.; Thomas, S. Electrical Properties of YBCO/Polymer Composites, 18th university conference on Glass; The American Ceramic Society: Rochester, US, 20–23 May 2007.
26. Lee, S.-L.; Chen, T.-M. Chin J Phys 1993, 31, 1175.
27. Rajesh, C.; Unnikrishnan, G.; Thomas, S. J Appl Polym Sci 2004, 92, 1023.
28. Sato, Y.; Furukawa J. Rubber Chem Technol 1963, 36, 1081.
29. Kerne, E. H. Proc. Phys. Soc. (B) 1956, 69, 802.
30. Quemada, D. Rheo Acta 1977, 16, 82.
31. Thomas, S. P.; Joseph, K.; Thomas, S. Mater Lett 2004, 58, 281.
32. Zakin, J. L.; Simha, R.; Hershey, H. C. J Appl Polym Sci 1966, 10, 1455.
33. V Krevelan, D. W.Properties of Polymers; Elsevier: Amsterdam, 1972.
34. Vollenburg, P. H. T.; De Hann, J. W. Polymer 1989, 30, 1663.
35. Matonis, V. A.; Small, N. C. Polym Eng Sci 1969, 9, 90.
36. Bruneel, E.; Persyn, F.; Hoste, S. Supercond Sci Tech 1998, 11, 88.
37. Joseph, P. V.; Joseph, K.; Thomas, S. Comp Inter 2002, 9, 213.

38. Bai, S. L.; Chen, J. K. Polym Inter 2001, 50, 222.
39. Pugh, H. L. D.; Chandler, E. F.; Holliday, L.; Mann, J. Polym Eng Sci 1971, 11, 463.
40. Francis, B.; Rao, V. L.; Thomas, S. Polym Eng Sci 2005, 45, 1645.
41. Goodier, J. N. J Appl Mech 1993, 55, 39.
42. Joel, F. R. Polymer Science and Technology; Prentice-Hall: India, 2004.
43. Nielsen, L. E. J Appl Polym Sci 1966, 10, 97.
44. Piggot, M. R.; Leidner, J. J Appl Polym Sci 1974, 18, 1619.
45. Nicholas, L.; Narkies, M. Polym Eng Sci 1971, 11, 194.
46. Gupta, A. K.; Purwar, S. N. J Appl Polym Sci 1984, 29, 3513.
47. Idicula, M.; Neelakandan, N. R.; Oommen, Z.; Thomas, S. J Appl Polym Sci 2005, 96, 1699.
48. Utracki, L. A. J Polym Sci Part B: Polym Phys 2008, 46, 2504.
49. Thomas, S. P.; Thomas, S.; Abraham, R.; Bandyopadhyay, S. Express Polym Lett 2008, 7, 528.